

# Impact analysis of adverse climate on long-haul 1280 Gb/s, hybrid multiplexed FST optical link

SHIVAJI SINHA<sup>1</sup>, KAMAL KISHORE UPADHYAY<sup>1</sup>, CHAKRESH KUMAR<sup>2,\*</sup>, GHANENDRA KUMAR<sup>3,\*</sup>

<sup>1</sup>JSS Academy of Technical Education, Noida, 20130, India

<sup>2</sup>University School of Information, Communication & Technology, Guru Gobind Singh Indraprastha University, New Delhi-110 078, India

<sup>3</sup>University School of Automation and Robotics, Guru Gobind Singh Indraprastha University, New Delhi-110 078, India

The growing demand for a high-speed Free Space Terrestrial Optical Link (FSTOL) under adverse atmospheric channel conditions is essential for next-generation wireless communication networks while retaining high throughput and reliability. In this research paper, we propose a cost-effective architecture of a high-speed multi-channel (32x40) Gb/s Dense Wavelength Division Multiplexing (DWDM)-based terrestrial optical link and investigate its performance under strong turbulent and different weather conditions such as haze, rain, and fog to identify the optimum link distance. Furthermore, the integration of higher-order modulation schemes like Quadrature Amplitude Modulation (16-QAM) along with the robustness of Orthogonal Frequency Division Multiplexing (OFDM) and DWDM multiplexing techniques helps to achieve a higher data rate and effective bandwidth utilization with low attenuation for longer link distances. The investigation dealt deep into performance metrics such as Bit Error Rate (BER), average received power, and optimum link distance in the adverse atmospheric weather scenario. The simulative result clearly shows the degraded signal quality below an acceptable threshold BER level of  $\leq 2 \times 10^{-3}$  at Optical Signal to Noise Ratio (OSNR) of 17 dB for the transmission range beyond 2 km, 0.5 km, and 0.4 km under dense haze, heavy rain, and dense fog conditions.

(Received October 23, 2024; accepted February 3, 2025)

**Keywords:** Atmospheric Turbulence, Bit Error Rate (BER), Free Space Terrestrial Optical Link (FSTOL), Eye diagram, Hermite Gaussian (HG), Mode division multiplying (MDM), Orthogonal Frequency Division Multiplexing (OFDM), Optical Signal to Noise Ratio (OSNR), Quadrature Amplitude Modulation (QAM)

## 1. Introduction

Free-Space Terrestrial Optical Link (FSTOL) system offers tremendous potential to meet the demand for higher data transmission rates for future spectrally efficient wireless networks. The FSTOL system offers advantages like enormous bandwidth, high channel capacity, immunity to electromagnetic interference, and security with a license-free spectrum [1,2]. These systems comprise of a tightly aligned Line of Sight (LOS) radio nodes, which optically modulate data using various modulation formats and transmit it over a complex free space link. The quality of the received data degrades at the receiver end and depends on different external limiting factors such as beam wander, scintillation, and severe attenuation levels due to dynamic weather conditions [3]. These variables result in a low Signal-to-Noise Ratio (SNR), which leads to reduced system performance and is characterised by weak signal intensity levels, skewed phase, and polarisation at the receiver end [4].

Different research papers have put forward numerous architectures of FSTOL systems in recent years to address these constraining variables and improve the data rate and spectral efficiency. To counter these atmospheric limitations, these architectures include various multiplexing techniques, such as Space Division

Multiplexing (SDM), Polarisation Division Multiplexing (PDM), and Dense Wavelength Division Multiplexing (DWDM). The performance of these FSTOL system designs has been evaluated in various weather conditions, including intense rainfall, dense fog, dusty environments, and hazy weather scenarios, and shows improved performance. However, these techniques perform poorly in strong turbulent and multipath fading channel conditions caused by atmospheric turbulence [5,6,7]. Another cost-effective transmission technique that exploits the eigenmode attributes of the spatial optical beam to transport distinct information over the same transmission link is Mode Division Multiplexing (MDM). Different optical signal processing methods were presented to generate multiplexed and demultiplexed laser modes using a spatial light modulator [8]. Researchers have also described the application of dual-fused fibre and photonic crystal fibre in high-speed MDM transmission. Multi-mode fibre (MMF) links can realise high-speed data transmission using linear polarised (LP) modes [9].

In recent years many research papers, have suggested Orthogonal Frequency Division Multiplexing (OFDM) as a more reliable and promising technique by integrating its distinct feature with optical wireless links to improve the transmitted range under multipath fading channels. Many research papers have investigated the MDM-OFDM based

FSTOL performance under various weather conditions. OFDM transmit high-speed data over a terrestrial optical wireless link using precisely spaced low-bit rate multiple subcarriers in the frequency domain [10]. The mapping of the bit stream over the large narrowband subcarriers helps to reduce the multipath fading and inter-symbol interference (ISI). It is not only a robust technique against multipath fading, but it also improves the data transmission rate and offers high spectral efficiency without any need for receiver equalization [11]. Different research articles have discussed multiplexing in phase, code, polarization, and wavelength to maximize the data carrying capacity and the transmission link range. Orbital Angular Momentum (OAM) has been reported as another technique that, along with channel coding can be used to compensate multipath channel fading and improve FSO system performance [12,13]. An ultra-high-speed, DWDM, 32-channel, hybrid fibre-based optical system has been implemented to transmit 320 Gb/s and 1280 Gb/s optically modulated data using On-Off Keying (OOK) and advanced modulation formats under dynamic turbulent, fog, and rain conditions, respectively. An impact of change in internal system parameters such as beam divergence and diameter of transmitter & receiver aperture has also been investigated on the system performance. The proposed system clearly indicates that the received signal quality falls significantly below an unacceptable value at transmission distances greater than 0.8 km, 1.4 km, and 1 km, respectively [14,15]. In recent years, researchers have incorporated a new approach based on Artificial Neural Network (ANN) and Support Vector Machine (SVM) to analyse and predict signal impairments at the optical recovery. A WDM-based 8-channel Ro-FSO system is designed to transmit 80 Gb/s phase shift keying (PSK)-modulated optical data under different haze and fog conditions. The proposed system has offered the best performance using the linear SVM technique in the estimation of the quality (Q) factor [16].

This research paper contributes to the design of a novel hybrid multiplexed FSTOL link that achieves a data

throughput of 1280 Gb/s with an optimum link distance considering a strong turbulent atmosphere with different weather conditions. The proposed design further integrates the OFDM technique into each channel to carry 40 Gb/s of 16-QAM modulated optical data, enhancing data rate, spectral efficiency, and resilience against various channel impairments like multipath propagation and dispersion. DWDM multiplexing maximizes the utilization of the available optical spectrum by multiplexing such 32-channels. The author's literature survey found no research article proposing such a hybrid FSTOL system.

The proposed research work is split into distinct sections, as follows: Section 2 presents an overview of the proposed hybrid multiplexed FSTOL system, including its full architecture design, system parameters, and signal modelling. Section 3 demonstrates the mathematical analysis of the optical atmospheric link model while Sections 4 and 5 conclude with an examination of the simulation findings and ideas for future enhancements to the proposed system design.

## 2. System architecture and signal modelling

A simplified block diagram of the proposed high-speed hybrid multiplexed FSTOL system is shown in Fig. 1. This system uses DWDM for both multiplexing and demultiplexing. The proposed system uses the 16-QAM modulation scheme to convert binary data into symbols. The system parameters that are used to design the proposed system are also summarized and summarized in Table 1. The hybrid multiplexed FSTOL system consists of three sub-systems: (i) An optical transmitter comprises of 32-channel DWDM multiplexer and with each channel using 16-QAM-OFDM, (ii) An optical channel, and (iii) optical receiver. Fig. 2 and Fig. 3 respectively, demonstrate the detailed structure of these subsystems operating at 40 Gb/s.

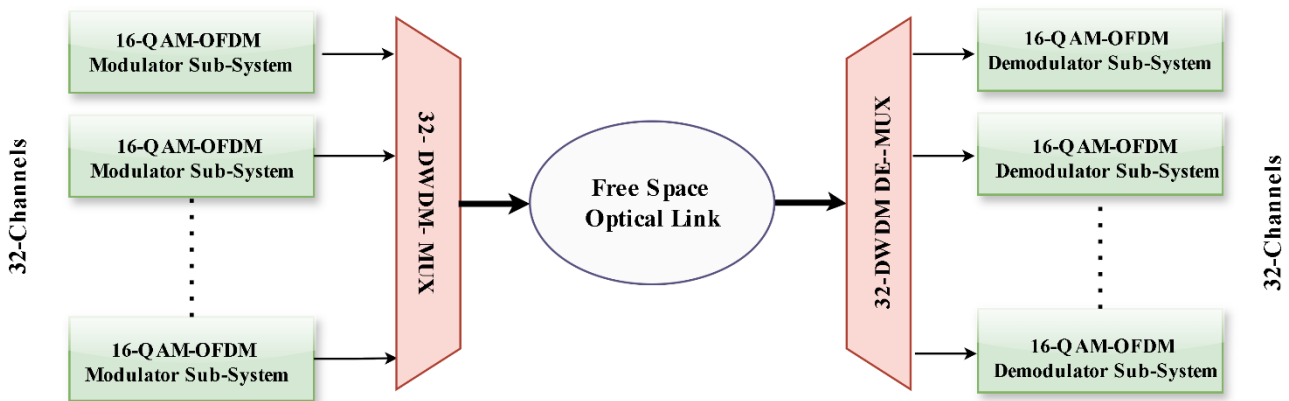


Fig. 1. Block diagram of the proposed multi-channel hybrid multiplexed system

Table 1. System parameters of the proposed system [17]

System Parameters	Symbols	Numerical Values
Optical Transmitter Parameters		
Optical power	$P_t$	10 dBm
laser linewidth	$\Delta f$	0.1 MHz
Data rate	$R_b$	40 Gb/s
Sequence length	l	65536
Sample/bit	s	32
Aperture diameter	$d_t$	10 mm
channel spacing	$\Delta f$	0.8 nm
Channels Wavelengths		
Channel Number		Frequency
Channel 1		1550.00 nm
Channel 8		1544.36 nm
Channel 16		1537.91 nm
Channel 32		1525.03 nm
FSO Channel Parameters		
Maximum link distance	L	10 km
RIS parameter	$C_n^2$	$5 \times 10^{-13} m^{-2/3}$
Maximum Atmospheric Attenuation Levels (dB/km)		
Clear sky		0.16
Dense haze		10
Heavy rain		27
Dense fog		340
Optical Receiver Parameters		
Aperture diameter	$d_r$	20 mm
Beam divergence	$\phi$	1 mrad
Photo detector dark current	$I_d$	10 nA
Photodiode Responsivity	A	1 A/W
Thermal noise power density	$N_0$	10 <sup>-22</sup> W/Hz
Load resistance	$R_L$	50 $\Omega$
Receiver bandwidth	B	20 MHz
Filter order	n	4
LPF cut off frequency	fc	1.8 GHz

Table 2. OFDM system parameters [17]

OFDM Parameters	Symbols	Numerical Values
No of data sub-carriers	N	512
IFFT points	m	1024
No of OFDM symbols	s	40
Cyclic prefix duration	Tc	0.8 $\mu$ s
Clipping noise variance	$\sigma_{clip}^2$	0.002
Utilization factor	GB	0.5
Average electrical losses/bit	GDC	0.6 dB

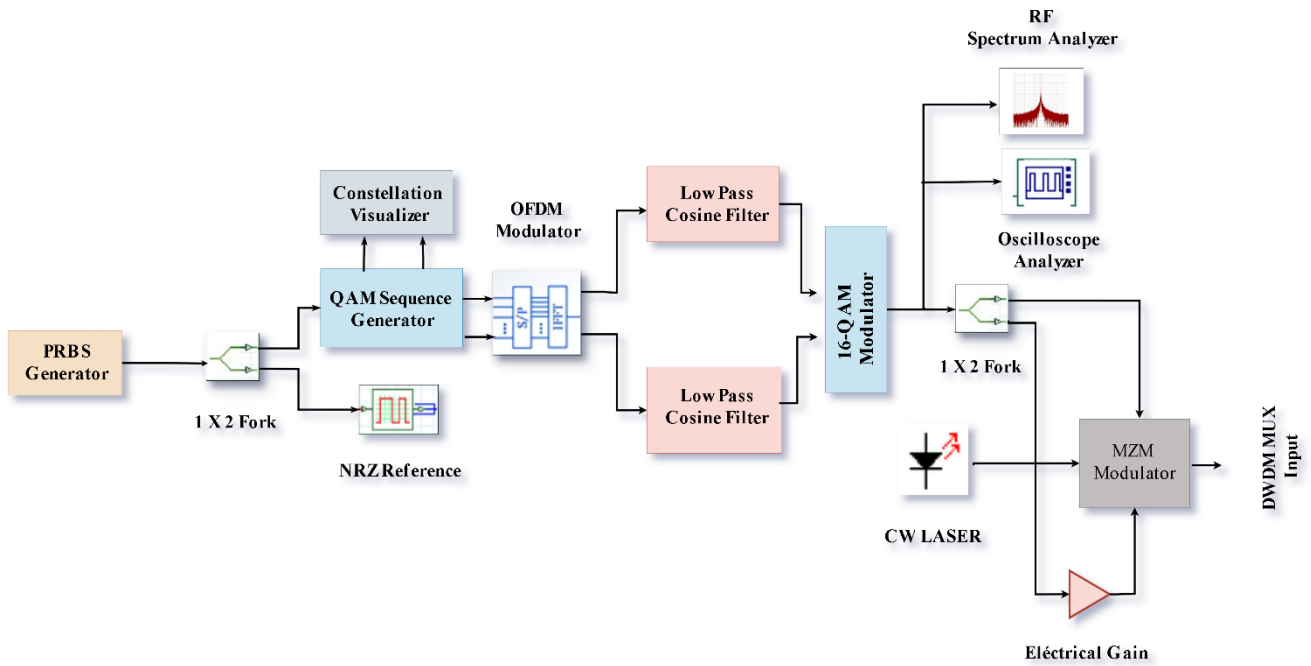


Fig. 2. Internal schematic circuit diagram for a single channel hybrid FSTOL transmitter subsystem

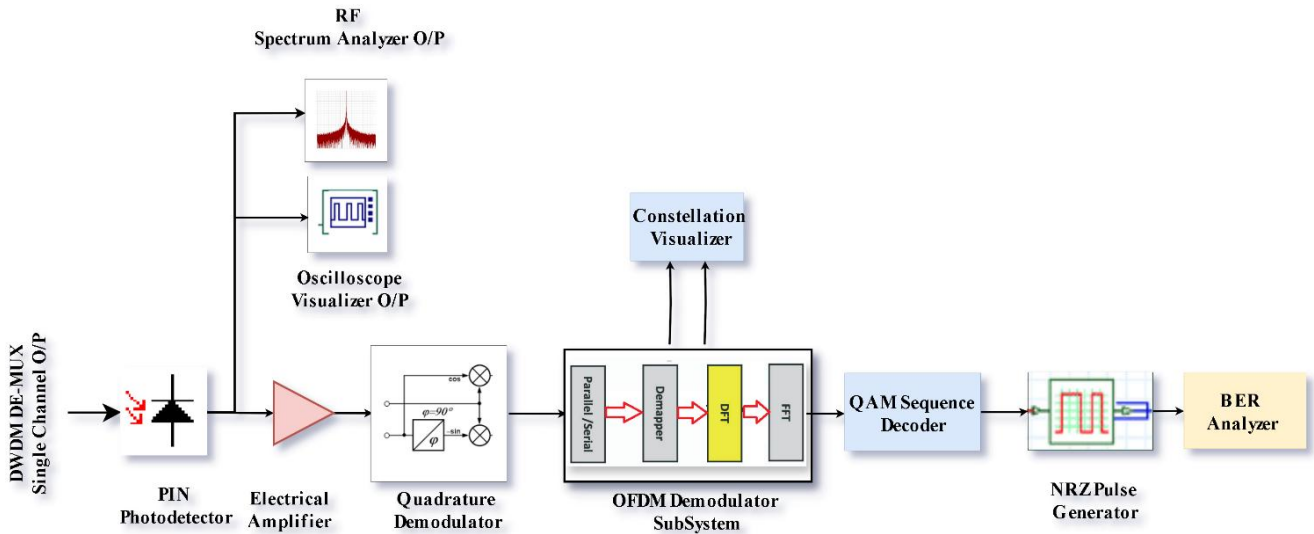


Fig. 3. Internal schematic circuit diagram for a single channel hybrid FSTOL receiver subsystem

The schematic design of a single channel 16-QAM-OFDM subsystem, as depicted in Fig. 2, consists of a pseudo-random bit sequence generator (PRBS) that generates binary data, first converting it into NRZ electrical format  $X_i(t)$ , and then mapping it onto a QAM modulated data  $M_i(t)$ , with 4 bits/symbol in the QAM sequence generator. This output from this QAM block comprises of in-phase (I) and quadrature phase signals (Q) components. The constellation visualizer is used to visualize I and Q phase components in terms of a constellation diagram after passing through coupled M-ary Raised Cosine Pulse generator. The output of the QAM block is then sent to the OFDM modulator to produce N

number of OFDM sub-carrier signals. The output from this OFDM block is represented by  $S_n(t)$  and expressed by Eq. (1) for  $0 \leq T \leq T_s$ . The OFDM parameters considered for the proposed system design are summarized in Table 2.

$$S_n(t) = \sum_{n=0}^{N-1} X_n e^{i(\omega_n + 2\pi f_c)t} = \sum_{n=0}^{N-1} X_n e^{[2\pi i(nf_s + f_c)t]} = \sum_{n=0}^{N-1} X_n e^{[2\pi i(\frac{n}{T_s} + f_c)t]} \quad (1)$$

where  $\omega_n$  and  $T_s$  are the orthogonal frequency and time period of OFDM signal respectively, and  $X_n = a_n + ib_n$  is the symbol of the  $n^{\text{th}}$  subcarrier while  $f_c$  is the carrier frequency used to maintain the orthogonality among the

OFDM sub-carriers [18,19]. This QAM-OFDM modulated electrical data is then optically modulated in LiNBO<sub>3</sub> dual arm Mach-Zehnder Modulator (MZM) block by using laser transmitter to produce optically modulated signal P(t) given by Eq. (2) for the  $b_3$  as a non-linear coefficient of Laser source while  $m_n$  is an optical modulation index, respectively

$$P(t) = P_t [1 + \sum_{n=0}^{N-1} m_n S_n(t) + b_3 (\sum_{n=0}^{N-1} m_n S_n(t))^3] \quad (2)$$

The DWDM block multiplexes these 32-channel output data to produce high-speed optical signal at data rate of 1280 Gb/s to transmit through the complex atmospheric optical link. The total power ( $P_{sum}$ ) of the transmitted DWDM multiplexed channel is given by  $P_{sum} = P_{ch} + \log(N)$ . Here,  $P_{ch}$  is the per channel power while  $N=32$  [20].

The signal propagated through the free space channel suffers intensity attenuation and phase distortion. The received optical power  $P_r(t)$  at the receiver end is given by Eq. (3), and the corresponding Link Margin (LM) by Eq. (4), respectively.

$$P_r = P_r \sigma_{att} L I + n(t) \quad (3)$$

$$LM = \frac{10 \log P_r}{s} \quad (4)$$

where  $\sigma_{att}$ , is the total atmospheric attenuation, and  $I$  instantaneous irradiance fluctuations at the receiver input while  $n(t)$  is the additive white Gaussian noise with zero mean and noise variance  $\frac{N_0}{2}$ . The parameter  $S$  represents the receiver sensitivity whose value is provided by the manufacturer and lies in the range of  $-20$  dBm to  $40$  dBm [21, 22].

The attenuated and distorted signal at the receiver end is given to the input of the DWDM de-multiplexer where each 32-channels optical data is separated and converted back to binary electrical information through a PIN photodiode detector using a coherent detection technique. This signal is further applied to the 16-QAM sequence decoder to visualize the distorted binary signal in the BER analyser to observe the system performance.

The scintillation and the atmospheric turbulence produce the intensity fluctuations and phase distortion in the received signal. Thus, the instantaneous current at the receiver end is written by

$$i(t, I) = I_0 [1 + \sum_{n=0}^{N-1} m_n S_n(t) + b_3 (\sum_{n=0}^{N-1} m_n S_n(t))^3] + n(t) \quad (5)$$

here  $I_0 = \rho L_{att} P_t$  is the average value of the instantaneous current  $i(t)$  with photodetector responsivity ( $\rho$ ) and the noise variance. The noise variance is expressed as

$$N_0 = \frac{4K_B T F}{R_L} + 2qI_0 + I_0 R_{IN} \quad (6)$$

where  $K$  is the Boltzmann constant, and  $R_L, B, F$ , and  $T$ , are load resistor across the photodetector, the receiver bandwidth, the noise figure, and the absolute temperature,

respectively. The parameters  $q$  and  $R_{IN}$  are the electronic charge and relative intensity of noise [4].

For the average value of optical noise =  $\left[ \frac{N_0}{T_s} \right]_{Av}$ , and intermodulation distortion =  $[\sigma_{IMD}^2]_{Av}$ , the instantaneous carrier-to-noise distortion ( $CNDR$ ) <sub>$n$</sub>  at the receiver for each OFDM subcarrier is denoted by Eq. (7) [23]

$$CNDR_n(I) = \frac{(m_n \rho L_{att} P I^2)}{2 \left( \left[ \frac{N_0}{T_s} \right]_{Av} + [\sigma_{IMD}^2]_{Av} \right)} \quad (7)$$

### 3. Optical turbulence model

Attenuation losses from the divergence and scattering of the transmitted optical beam may restrict the transmission range of the hybrid-FSTOL system. However, channel attenuation and the non-uniform refractive index structure (RIS) of the atmospheric layers reduce the range under unfavourable weather conditions such as scintillation and atmospheric turbulence. These processes can cause phase changes in the received optical signal [17]. Particularly in intense fog conditions, the signal's scattering and absorption diminish the link. Scattering and absorption primarily reduce the link under heavy rain scenarios [25]. The proposed system operates at an optimal shorter wavelength to prevent these losses, while adjusting the transmitted beam's phase and using multipath strategies can reduce the impact of scintillation and beam wandering, thereby enhancing the system's reliability [1]. In the proposed system, we have considered the Kim Model to examine the atmospheric losses due to various weather conditions. For a fixed value of  $q$  in this model, these losses decrease with increasing wavelength  $\lambda$ . At wavelength  $\lambda=1550$  nm, the visibility for specific attenuation levels (dB/km) is listed for various weather conditions in Table 3 [24].

Further, the RIS ( $C_n^2$ ) and the Rytov ( $\sigma_R^2$ ) are the coefficients that characterize the turbulence strength and hence determine the turbulence regime. These parameters are defined by Eq. (8) and Eq. (9), respectively.

$$C_n^2 = \left( 86 \times 10^{-6} \times \frac{P}{T^2} \right)^2 R_T^2 \quad (8)$$

$$\sigma_n^2 = 1.23 C_n^2 k^7 L^{\frac{11}{6}} \quad (9)$$

Table 3. Attenuation level for different weather [24]

Weather	Attenuation (dB/km)	Visibility (km)
Heavy Fog	340	0.16
Heavy Dust	242	0.20
Dust	10	0.5
Rain	7	1
Partial Cloud	2	4
Clear	0.6	23

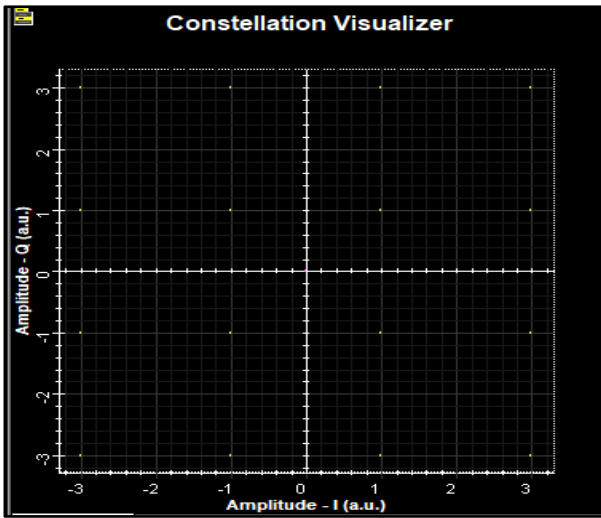
where  $P$ , and  $R_T^2$  represent the air pressure in millibar and temperature structure coefficient, whereas optical wave

number and propagation link distance are denoted by  $k = \frac{2\pi}{\lambda}$ , and  $L$ , respectively. The range of  $C_n^2$  varies from  $10^{-13} m^{-2/3}$  to  $10^{-17} m^{-2/3}$  for strong to weak turbulence regime, respectively.

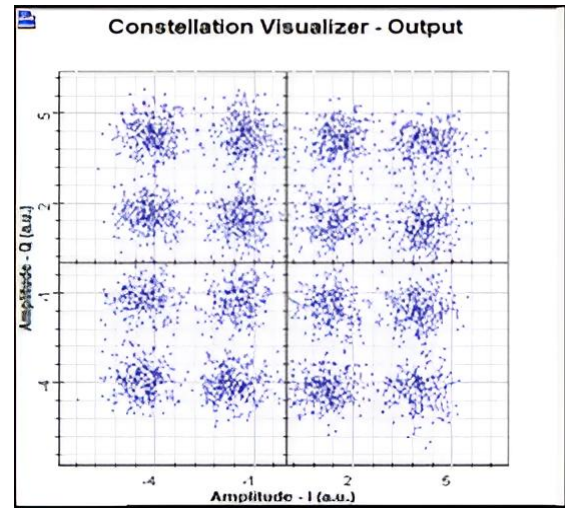
#### 4. Results and discussions

This section examines the findings of the proposed hybrid-multiplexed FSTOL system for fixed strong turbulence ( $C_n^2 = 5 \times 10^{-5} m^{-2/3}$ ) and different weather conditions like haze, fog, and rain, including clear sky.

The performance of the proposed FSTOL system is assessed in terms of log BER vs. threshold OSNR sensitivity for various link distances and received optical power under three different weather scenerios. The simulation setup is designed in the Opti system platform, as shown in Fig. 2 and Fig. 3, respectively, and the obtained data is analyzed using the Matlab tool. Tables 1 and Table 2 also demonstrates the summary of proposed system modelling parameters. During the simulation process and hence result analysis, the presence of various impediments such as trees, birds, buildings, and signboards is not assumed in the proposed system.



(a)

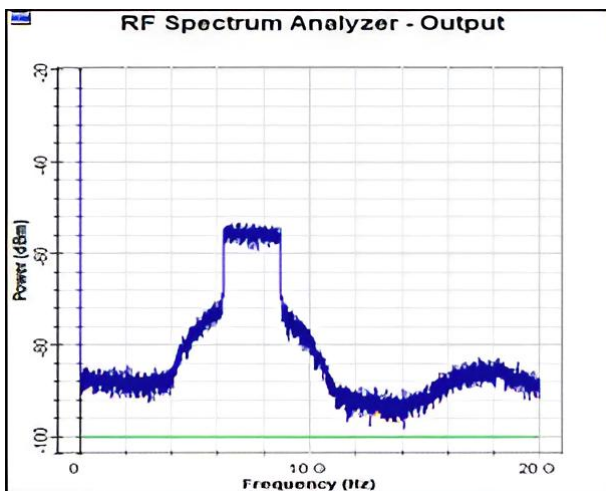


(b)

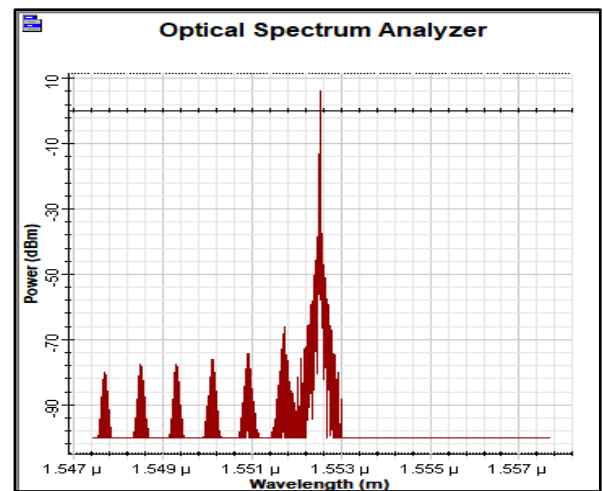
Fig. 4. Symbol constellation (a) before and (b) after the OFDM sub-system at the transmitter section

The system losses, coupling, geometrical, and misalignment losses, are all assumed to be zero, while multipath channel fading is assumed to be constant from one frame to the next across the coherence time. The constellation diagram for the in-phase and quadrature-phase components after the 16-QAM and after OFDM modulator blocks are shown in Fig. 4(a) and Fig. 4(b),

respectively, whereas Fig. 5(a) and Fig. 5(b) shows their corresponding RF and optical OFDM spectrums generated by the two arm  $\text{LiNbO}_3$ -MZM optical modulator. The Fig. 5(b) clearly demonstrates the maximum optical power concentration near the wavelength of  $1.55 \mu\text{m}$ .



(a)



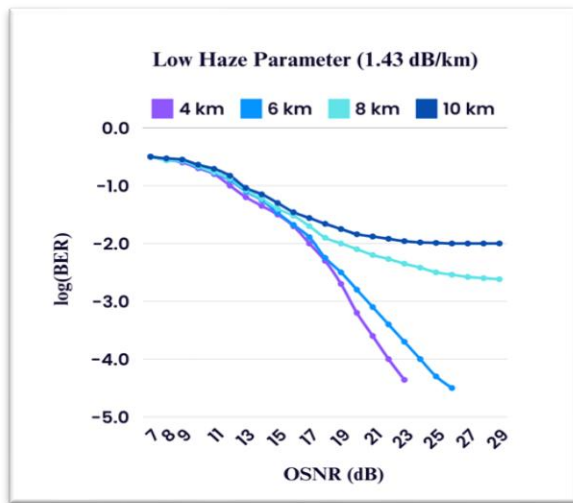
(b)

Fig. 5. Emissive RF and optical spectrums of the hybrid-multiplexed FSTOL system

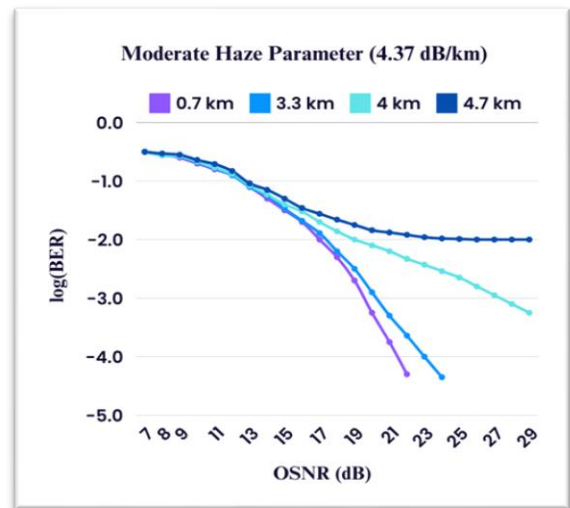


Fig. 6 presents the investigation of the proposed system's performance at an attenuation level of 0.16 dB/km under clear sky condition for B<sub>2</sub>B conditions. We evaluate the link performance for transmission ranges of 5 km, 16 km, 20 km, and 25 km, respectively. The proposed system performs excellently for the BER limit  $2 \times 10^{-3}$  15 km optimum transmission range, with an OSNR of 17 dB, which is comparatively much better than achieving 10 km in [27] for the QAM-4 at OSNR of 14.3 dB and 1.2 km for QAM-16 modulation format at OSNR of 23.5 dB, respectively, at 100 Gb/s data transmission rate. In order to achieve exceed this 15 km range, the OSNR must rise above 17 dB, which is why the proposed system performs poorly at the given threshold limit.

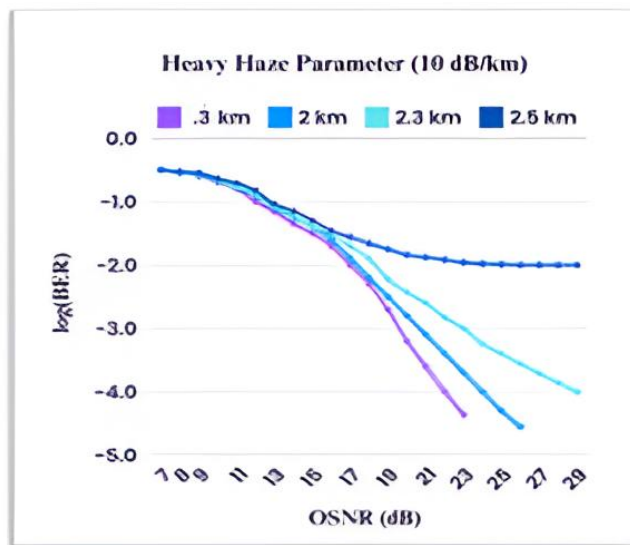
Fig. 6. BER vs. OSNR graph for B<sub>2</sub>B link under clear sky



(a)



(b)

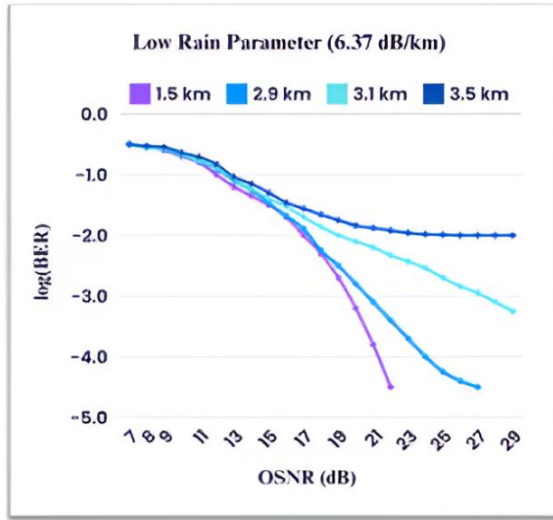


(c)

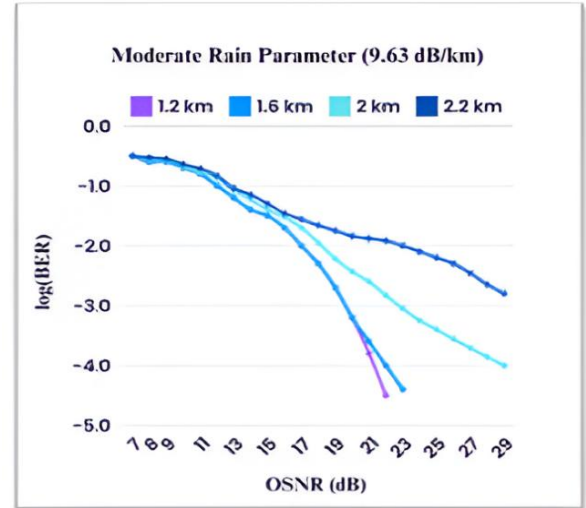
Fig. 7. BER vs. OSNR graph for B<sub>2</sub>B link (a) low (b) moderate (c) heavy haze conditions

The attenuation owing to atmospheric absorption and scattering losses is examined for mild to dense haze weather conditions as presented in Fig. 7. Each graphical result, shown here plots the simulated log (BER) numerical values with respect to OSNR ranging from 1dB to 10 dB for different transmission links ranging from 0.4 km to 10 km. It is noted that with the increase in link distance, the BER performance of the system decreases and reaches to value of  $-5$  at an OSNR of 29 dB. This is due to the decrease of optical power nonlinearly with the

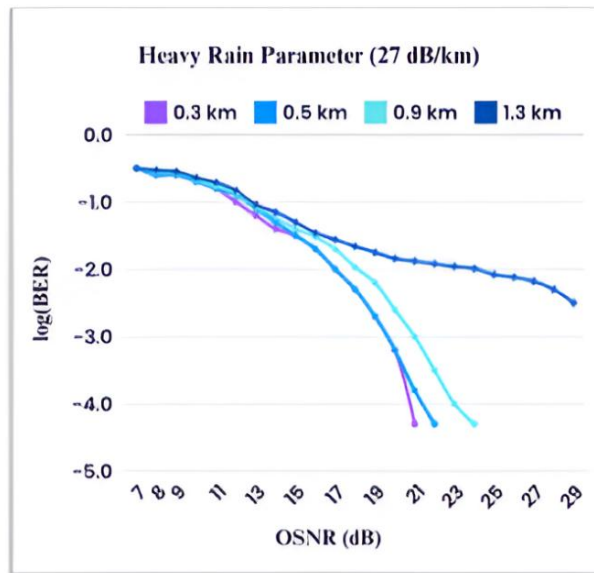
square of the increase in link distance, i.e., at higher link distance, more amount of power is required to achieve the same performance of the system. To achieve a threshold BER limit [26] of  $\leq 2 \times 10^{-3}$  at fixed OSNR of 17 dB, the optimum link distance achieved is 6 km at low haze (attenuation level of 1.43 dB/km), while the minimum link distance achieved is 2 km under dense haze (attenuation level of 10 dB/km) conditions, respectively.



(a)



(b)



(c)

Fig. 8. BER vs. OSNR graph for B<sub>2</sub>B link (a) low (b) moderate (c) heavy Rain conditions

This clearly indicates that to achieve the same system performance, the required OSNR increases by 0.2 dB to obtain 2 km, 1.6 km, and 1.7 km additional transmission range in mild, moderate and dense haze weather,

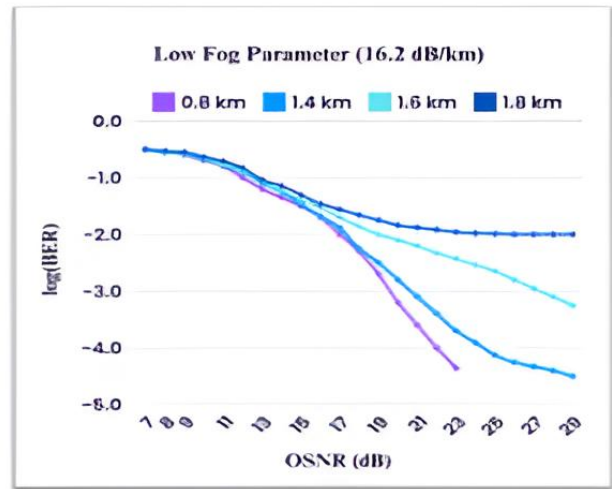
conditions respectively. Hence the optimum transmission range achieved are 6 km at 1.43 dB/km, 3.3 km at 4.37 km, and 2 km respectively for 10 dB/km attenuation levels. The results from the simulation are much better

than those in Ref. [27], which shows that the transmission range is 5.5 km for low haze, 3.6 km for mild haze, and 2 km for heavy haze, with a higher OSNR value of 23 dB and a lower data rate.

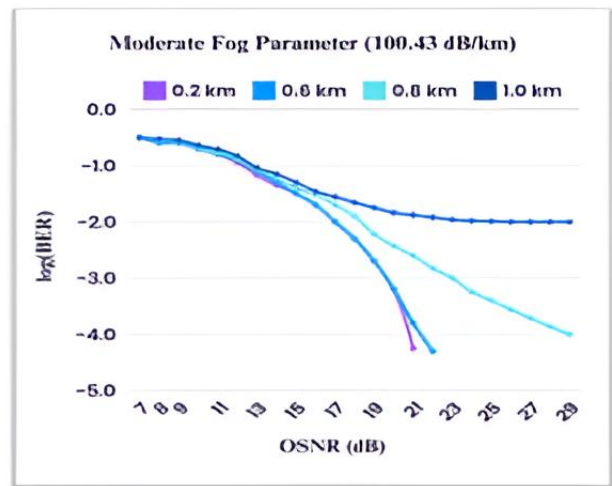
Fig. 8 illustrates the measured system BER performance relative to the increasing OSNR values under the impact of for light rain to heavy rain scenario. It demonstrates that at an OSNR of 17 dB, the realized transmission range decreases by 0.3 km and 1.2 km for moderate and heavy rain, respectively as opposed to 1.5 km in light rain conditions. At threshold BER of  $2 \times 10^{-3}$ , 0.2 dB, 2.2 dB and 6.8 dB, an additional power penalty is required to achieve additional link distances of 1.4 km, 1.6 km, and 1.9 km, respectively, at a fixed attenuation level of 6.37 dB/km, while the same power penalty is required to obtain the link distances of 0.4 km, 0.8 km, and 1 km respectively at an attenuation of 9.63 dB/km (Fig. 8(b)). The worst system performance is obtained under heavy rain, where the achieved transmission range are 0.2 km, 0.6 km, and 1 km respectively as depicted in Fig. 8(c). The proposed system offers its optimum performance of 2.9 km in low rain, 1.6 km in moderate rain, and 0.5 km in heavy rain conditions respectively below the threshold BER limit at 17 dB OSNR. The transmission link distance achieves 3.2 km for low rain, 2.2 km for medium rain, and 1.1 km for heavy rain, with an almost 3 dB increase in OSNR value compared to the simulation results obtained for the proposed system, according to Ref. [17], and Ref. [27].

To analyze the log BER vs. link distance performance of the proposed system for fog scenario, all the simulation parameters are kept according to Table 1 and Table 2, respectively, except the attenuation levels, which are 16.2 dB/km, 100.43 dB/km, and 340 dB/km for low, moderate, and very dense fog conditions, as depicted in Fig. 9. The system's performance significantly deteriorates when comparing the achieved link distance to various haze and rain attenuation levels, primarily because of reduced visibility, particularly in extremely dense fog conditions. As shown in Fig. 8, the link distance reduces by 0.6 km in dense fog condition compared to mild fog scenario at required OSNR of 17 dB. To achieve a threshold limit of  $2 \times 10^{-5}$ , 0.6 km, 0.8 km, and 1 km transmission range is more archived, but at the cost of 0.2 dB, 2.2 dB, and 6.8 dB power penalty, at 17 dB OSNR under mild fog condition shown in Fig. 9(a). Similarly, 0.4 km, 0.6 km, and 0.8 km more link distance are archived at the cost of same power penalty in moderate fog condition shown in Fig. 9(b) compared to mild fog case, while for the very heavy dense fog condition as illustrated in Fig. 9(c), the performance is worst and 0.1 km, 0.2 km, and 0.3 km more link distances are noted compared to mild case. Hence the proposed system depicts the best performance of 0.8 km at attenuation level of 16.2 dB/km for mild fog case. The proposed system performs much better even under very harsh attenuation levels as compared to those considered in Ref. [14] and Ref. [24]. As mentioned in Ref. [13], the maximum link distance obtained is 0.4 km for the attenuation level of 90 dB/km at an OSNR of 22 dB and a 320 Gb/s data transmission rate, whereas in the

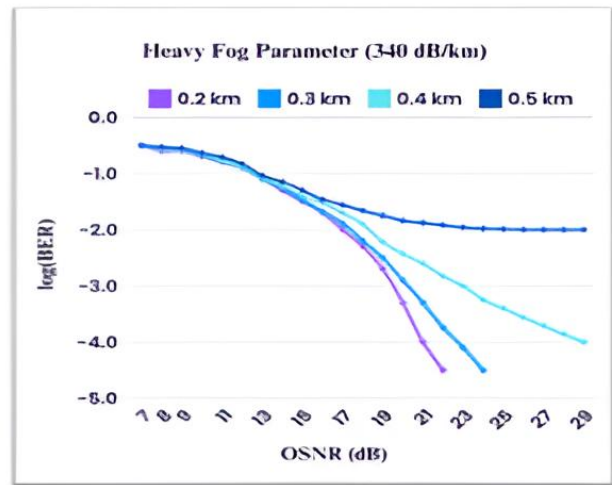
proposed system, the optimum link distance is 0.3 km for the attenuation level of 340 dB/km and an OSNR of 17 dB at a 1280 Gb/s data transmission rate.



(a)



(b)



(c)

Fig. 9. BER vs. OSNR graph for B2B link (a) low (b) moderate (c) heavy Fog conditions (color online)

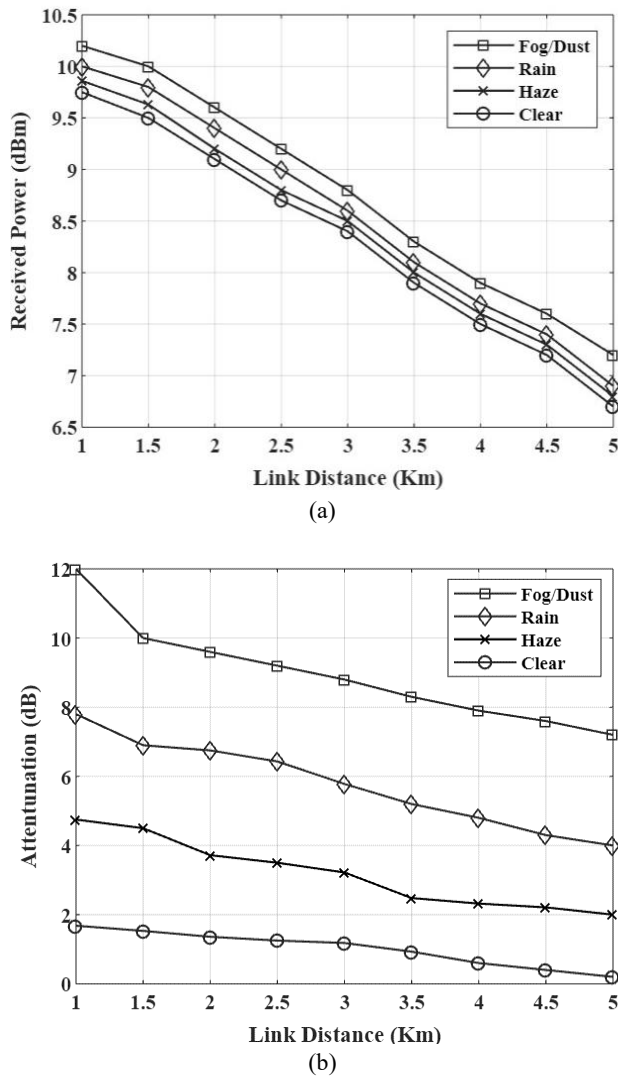


Fig. 10. (a) Received power and (b) attenuation vs. link distance under different weather conditions

Fig. 10(a) and Fig. 10(b), represent the proposed system link performance in terms of received signal power and attenuation levels as a function of link distance which decreases at the receiver aperture with the link distance, i.e., different weather conditions can significantly impact the signal quality. It is noticed that to reach a link distance of 3 km, a 8.386 dBm power is required in clear sky condition whereas 0.110 dBm power in haze, 0.179 dBm power in rain and 0.400 dBm additional power in dense fog condition as compared to clear sky. Similarly, for the same 3 km transmission range, the atmospheric attenuation levels increase from 1.723 dB in clearly sky to 4.875 dB in haze, 5.998 dB in rain and 8.889 dB under dense fog weather conditions. This means in any case, the proposed system performs worst in dense fog conditions, respectively.

## 5. Conclusions

This research work presents a robust analysis simulative investigation of a 32-channel high-speed, hybrid-multiplexed FSTOL system, which integrates OFDM and 16-QAM modulation, along with a coherent detection technique, across various weather conditions. Moreover, the proposed system supports a 1280 dB/s transmission rate for the acceptable threshold BER limit at  $\leq 17$  dB OSNR, maintaining the strong turbulence condition. The optimal link distance varies from 0.3 km to 15 km depending on different attenuation levels corresponding to different weather conditions. The maximum link distance achieved is 15 km for clear sky condition, while 2 km, 0.5 km, and 0.3 km under worst weather scenario of haze, rain and fog conditions. Hence, the proposed system has the capability to support fronthaul or backhaul links in future high-speed wireless networks at minimal cost. Furthermore, there is still scope to improve the performance of the system by incorporating various fading mitigating techniques such as adaptive coding, diversity schemes, and aperture averaging.

## References

- [1] S. A. Al-Gailani, M. F. M. Salleh, A. A. Salem, R. Q. Shaddad, U. U. Sheikh, N. A. Al-Gilani, T. A. Almohamad, *IEEE Access* **9**, 7353 (2021).
- [2] A. Jahid, M. H. Alsharif, T. J. Hall, *Journal of Network and Computer Applications* **200**, 103311 (2022).
- [3] A. Sharma, S. Kaur, N. Nair, K.S. Bhatia, *Optik* **257**, 168809 (2022).
- [4] H. Singh, N. Mittal, R. Miglani, H. Singh, G. S. Gaba M. Hedabou, *IEEE Photonics Journal* **13**(5), 1-12 (2021).
- [5] V. S. Pandi, M. Singh, A. Grover, J. Malhotra, S. Singh, *International Journal of Communication Systems* **35**(6), 1-13 (2022).
- [6] Anuranjana, Sanmukh Kaur, Rakesh Goyal, Sushank Chaudhary, *Optik* **257**, 168809 (2022).
- [7] S. Chaudhary, L. Wuttisittikulij, J. Nebhen, X. Tang, M. Saadi, S. A. Otaibi, A. Althobaiti, A. Sharma, S. Choudhary, *Frontiers in Physics* **9**, 1-7 (2021).
- [8] H. Singh, N. Mittal, R. Miglani, A. K. Majumdar, *Third South American Colloquium on Visible Light Communications (SACVLC)*, Toledo, Brazil, 01-06 (2021).
- [9] Nitin Bhatia, Kailash C. Rustagi, Joseph John, *Optics Express* **22**(14), 1684 (2014).
- [10] S. Boobalan, S. A. Prakash, M. Angurala, J. Malhotra M. Singh, *Wireless Personal Communications* **122**, 3137 (2022).
- [11] R. Miglani, J. S. Malhotra, *Wireless Personal Communications* **109**, 415 (2019).
- [12] S. Du, T. Wang, Q. Yang, B. Li, 2022 IEEE 10th International Conference on Information, Communication and Networks (ICICN), Zhangye, China, 142 (2022).

- [13] S. Cai, W. Sheng, Z. Zhang, *Optics Express* **31**(19), 30446 (2023).
- [14] A. Sharma, S. Kaur, S. Chaudhary, *Optical and Quantum Electronics* **53**(239), 1 (2021).
- [15] A. Sharma, S. Kaur, *Optik* **248**, 168135 (2021).
- [16] S. Kaur, A. Sharma, *J. Optoelectron. Adv. M.* **25**(9-10), 444 (2023).
- [17] D. Kakati, S. C. Arya, *Optik* **178**, 1230 (2019).
- [18] N. Kumar, A. Sharma, V. Kapoor, *Journal of Optical Communications* **35**(2), 151 (2014).
- [19] A. El-Rahman, El-Fikky, S. Abdallah. Ghazy, S. Haitham, Khallaf, M. M. Ehab, M. H. Hossam, Shalaby, H. A. Moustafa, *Applied Optics* **59**, 1896 (2020).
- [20] H. A. Willebrand, B. S. Ghuman, *IEEE Spectrum* **38**, (8), 40 (2001).
- [21] R. Ibragimov, V. Fokin, *Proceedings of the 2014 12<sup>th</sup> International Conference on Actual Problems of Electronics Instrument Engineering (APEIE)*, IEEE, 2014.
- [22] S. Parkash, A. Sharma, H. Singh, H. P. Singh, *Advances in Optical Technologies* (2016).
- [23] S. Chaudhary, A. Amphawan, K. Nisar, *Optik* **125**, 5196 (2014).
- [24] M. Uysal, J. Li, M. Yu, *IEEE Transaction of Wireless Communication* **5**(6), 1229 (2006).
- [25] S. H. Alnajjar, S. Esraa Zuhair, *IOP Conference Series: Materials Science and Engineering* **1105**, 012035 (2021).
- [26] J. Karaki, E. Pincemin, D. Grot, T. Guillosoou, Y. Jaouen, R. Le Bidan, *Optics Express* **21**(14), 16982 (2013).
- [27] M. Singh, J. Malhotra, M. S. Mani Rajan, D. Vigneswaran, M. H. Aly, *Alexandria Engineering Journal* **60**(1), 785 (2021).

---

\*Corresponding author: ghanendra.usar@ipu.ac.in,  
chakreshk@ipu.ac.in